Dynamic stiffness in whirl and whip

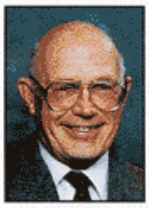

by Donald E. Bently
Chairman of the Board of Directors and Chief Executive Officer, Bently Nevada Corporation
President, Bently Rotor Dynamics Research Corporation

and Charlie Hatch, Rett Jesse and Joseph Whiteley
Bently Nevada Technical Training Department

When a fluid, either liquid or gas, occupies the space between two concentric cylinders, one rotating and one stationary, the fluid is set into motion in the gap. This can happen in rotating machinery in fluid-lubricated bearings, seals, around pump impellers, or in any fluid filled gap between rotor and stator. In the following article, we will primarily discuss fluid-lubricated bearings of basic cylindrical shape. However, everything written here about bearings also applies to seals, pump impellers, and any other region in a machine where there is fluid in a small clearance between a rotor and a stator.

In a fully lubricated fluid bearing, the fluid velocity at the surface of the bearing is zero, while the fluid velocity at the surface of the rotor is equal to the rotor surface speed. The oil near the rotor surface moves at a slightly slower velocity that continues to decrease with the distance from the rotor and reaches zero at the bearing surface. It is easy to see that the fluid must have some overall average velocity which is less than the rotor speed, and that the faster the rotor turns, the faster the fluid average velocity must be. In fact, previous work [1] has shown that the fluid circumferential average angular velocity in the bearing can be expressed as $\lambda\Omega$, where λ is the Fluid Circumferential Average Velocity Ratio, and Ω is the rotor rotative speed. The value of λ is a fraction, usually a little less than 1/2. In other words, the fluid circulates around the bearing with an average angular velocity typically less than 1/2 of the rotor speed, although λ can vary from as low as 0.05 to, rarely, greater than 1. Higher values of λ are usually attributed to pre-swirling of the fluid coming into the bearing.

If a radial load is applied to a rotor operating in the center of a fluid-lubricated bearing, the rotor will be displaced from the center of the bearing. The reduced

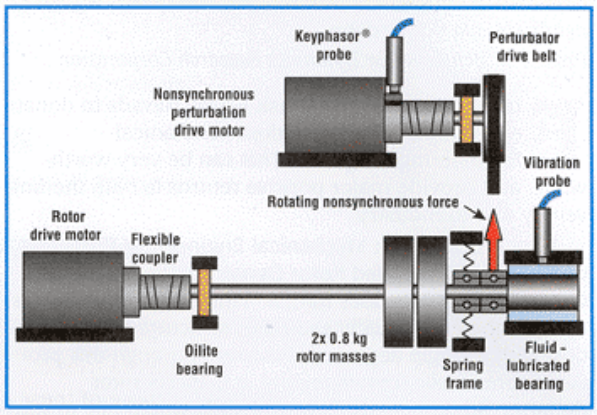

Figure 1. Experimental rotor rig. A separately mounted motor drives a perturbator with constant amplitude, rotating force which is attached to a rotor shaft.

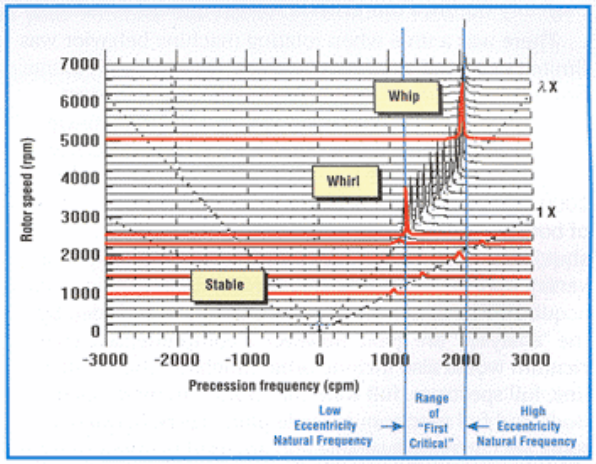

Figure 2. Full spectrum cascade plot of startup of rotor test rig. The rotor becomes unstable in whirl at approximately 2300 rpm. Transition to whip occurs at about 4500 rpm. The rotor speeds at which nonsynchronous perturbations were done are shown in red.

clearance on one side will restrict the flow of fluid around the journal bearing clearance. Because of this restriction, the fluid has to slow down as the available flow area gets smaller. As the fluid slows down, the pressure in this region increases. The pressure exerts a force on the rotor. This force can be separated into a *radial* part, which points back toward the center of the bearing, and a *tangential* part, which acts at 90° to the radial force, in the direction of fluid flow. Both the radial and

tangential forces are proportional to the displacement of the rotor from the center of the bearing. Thus, the lubricating fluid acts like a spring with a complex stiffness, and we refer to the radial part of the fluid wedge stiffness as the *Spring Stiffness* and the tangential part of the fluid wedge stiffness as the *Tangential Stiffness*. It is this complicated spring effect which provides the primary support for the rotor. The rotor and the fluid pressure "wedge" move until the fluid spring forces in the bearing exactly balance the radial load applied to the rotor (primarily gravity for a horizontal machine), and the rotor settles into an equilibrium position.

If the rotor is disturbed from the equilibrium position, the force due to the Tangential Stiffness tries to push the rotor in a tangential direction. The force due to the Spring Stiffness tries to return the rotor to the original position. However, the tangential motion produced by the tangential force prevents that from happening immediately, because the rotor inertia tries to keep things moving in that direction. Because of these effects, the rotor orbits around the equilibrium position. The viscous damping of the bearing fluid produces a force that opposes the velocity of the rotor, and the orbit spirals back to the equilibrium position. It is the complicated effect of these forces that maintains rotor stability. If these forces get out of balance, the rotor might continue to orbit about the equilibrium position. In fact, this is what happens with fluid instability: the instability is caused by particular relationships between the Spring Stiffness, the rotor inertia (which produces a *Mass-Related Stiffness*), the viscous damping force (which produces a *Damping-Related Stiffness*), and the Tangential Stiffness.

There is another way to look at what is going on. Because we are talking about *dynamic* motion, the rotor system behavior we have been talking about is best described by the *Dynamic Stiffness*. The Dynamic Stiffness of a simple rotor system is given by [2]

$$\vec{K}_{DS} = K - M\omega^2 + jD\omega - jD\lambda\Omega \qquad (1)$$

where the four terms to the right of the equal sign are the Spring Stiffness K, the Mass-Related Stiffness $-M\omega^2$, the Damping-Related Stiffness $+jD\omega$, and the Tangential Stiffness $-jD\lambda\Omega$.

The j in the equation is $\sqrt{-1}$, which means that the directions for these stiffness terms are at 90° from the other stiffness terms. M is the rotor mass, D is the bearing viscous damping, and ω is a term that represents the frequency of precession (or orbiting), which may be different from the rotation speed, Ω. λ is the Fluid Circumferential Average Velocity Ratio.

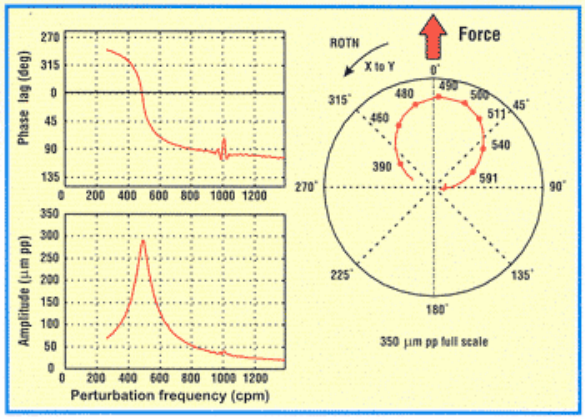

Figure 3. Bode and polar plot of the response to a nonsynchronous perturbation at a rotor speed of 1000 rpm. The phase of the force is 0° relative to the vertical probe at the moment the Keyphasor event occurs. The horizontal axis of the Bode plot and the labels on the polar plot are perturbation frequencies in cpm.

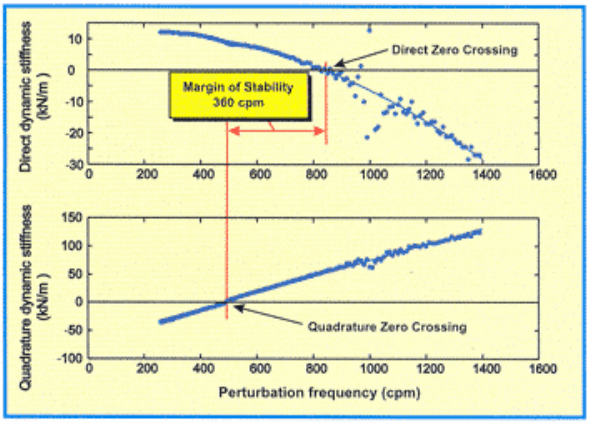

Figure 4. Dynamic Stiffness plots of the data from Figure 3. Direct Dynamic Stiffness appears in the upper plot, and Quadrature Dynamic Stiffness appears in the lower plot. Rotor speed is 1000 rpm in stable operation. The data appears as dots, and parabolic and linear curve fits have been applied. The zero crossings of the Direct and Quadrature Dynamic Stiffness are widely separated, and the Margin of Stability is 360 cpm.

The Dynamic Stiffness is actually the denominator of the general, nonsynchronous, rotor response equation:

$$\vec{R} = \frac{\vec{F}}{\left[K - M\omega^2 + jD(\omega - \lambda\Omega)\right]} \qquad (2)$$

where $\vec{F}$ is the amplitude and phase of the force applied to the rotor system, and $\vec{R}$ is the amplitude and phase of the precession, or orbiting of the rotor system. Equation (2) shows that the Dynamic Stiffness controls the amplitude and phase of the response a rotor system that is subjected to a rotating force, $\vec{F}$.

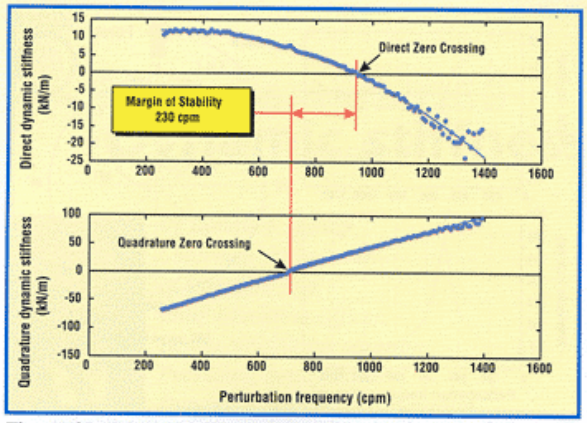

Figure 5. Dynamic Stiffness plots with the rotor operating at 1450 rpm in stable operation. The Margin of Stability has decreased to 230 cpm.

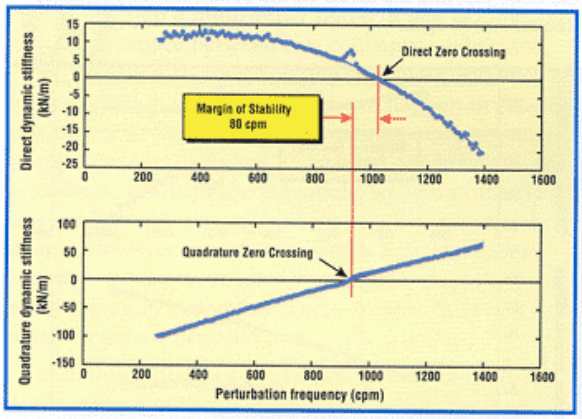

Figure 6. Dynamic Stiffness plots with the rotor operating at 1900 rpm in stable operation. The Margin of Stability has decreased to 80 cpm.

In Equation (2), the Spring Stiffness and the Mass-Related Stiffness form the *Direct Dynamic Stiffness*. It is called *Direct* because the Direct Dynamic Stiffness acts directly along the line of action of the force $\vec{F}$. Also, the Damping-Related Stiffness and the Tangential Stiffness have been combined into the *Quadrature Dynamic Stiffness*. It is called *Quadrature* because, as indicated by the j, it acts at 90° to the line of action of the force.

When the Damping-Related Stiffness $jD\omega$ is equal in magnitude to the Tangential Stiffness $-jD\lambda\Omega$, *the Quadrature Dynamic Stiffness* becomes zero. Also, when the Spring Stiffness K is equal in magnitude to the Mass-Related Stiffness $-M\omega^2$, the Direct Stiffness becomes zero.

For a stable rotor system, the Direct and Quadrature Dynamic Stiffnesses are *not* zero at the same frequency, and the difference in frequency between the zeros of the Direct and Quadrature Dynamic Stiffnesses is referred to as the *Margin of Stability*. The Dynamic Stiffness of a stable rotor system and its Margin of Stability is shown in Figure 4.

If both the Direct Dynamic Stiffness *and* the Quadrature Dynamic Stiffness become zero *at the same frequency*, then the denominator of Equation (2) goes to zero, and there is nothing to restrain the amplitude of vibration of the rotor. This is what happens at the Threshold of Stability, the rotor speed at which the rotor starts into fluid instability. At that point, the rotor begins whirling at the modified natural frequency of the rotor system.

But, what happens to the Dynamic Stiffness and the Margin of Stability as the rotor speed increases beyond the Threshold of Stability? Do the zero crossings of the Dynamic Stiffnesses stay together? Or, do they separate? Is the Dynamic Stiffness behavior in whirl different from that in whip? (Refer to Figure 2, which shows both whirl and whip, and the sidebar (page 9), "The difference between whirl and whip.")

The experiment

In order to explore the Dynamic Stiffness of the rotor system while operating in whip and whirl, it would be necessary to perform a nonsynchronous perturbation of the rotor system while the rotor operated at a constant speed in whirl or whip. An experimental rotor rig was assembled with a layout like that shown in Figure 1. The rotor system was designed with two 0.8 kg (1.8 lb) masses in order to have a relatively low instability threshold speed. This would allow oil whirl to occur near 2000 rpm. The masses were positioned about 6 cm (2.4 in) from the fluid-lubricated bearing on a 10 mm (0.39 in) diameter shaft with a span between the bearings of 42 cm (16.5 in). This ensured a transition to oil whip (which is associated with the rotor bending mode) at less than 5000 rpm. The rotor was driven by a 1/10 hp electric motor with a variable speed controller. A spring frame was installed to provide a force that would cancel the gravity load on the rotor.

A constant force perturbator was attached to the rotor as closely as possible to the fluid-lubricated bearing. The perturbator was designed to produce a rotating force of constant amplitude, 0.13 kg (0.29 lb) at a variable rotation frequency. Power to the perturbator was supplied by a separately mounted 1/10 hp, electric motor with a separate speed controller. A Bently Nevada Keyphasor® probe was installed on the perturbator motor to provide a once-per-turn phase reference pulse. A flexible, toothed drive belt transmitted the motor power to the perturbator through a 1:1 pulley system. The teeth on the drive belt served to maintain the correct phase relationship throughout the experiment. The

perturbator was constructed so it would isolate drive belt loads and the mass of the perturbator from the rotor shaft.

During the experiments, the spring frame was carefully adjusted to position the rotor journal in the center of the fluid-lubricated bearing. The bearing was constructed of a transparent material through which the journal and oil film could be seen. It was supplied with SAE 10 weight oil through four radial ports at a pump outlet pressure of 14 kPa (2.0 psi). The oil was mixed with a dye that allowed visual inspection of the condition of the oil film during the experiment. The oil temperature (in a holding tank after exiting the bearing) was 27° C (81° F) during the whirl experiment and approximately 44° C (111° F) during the whip experiment. No attempt was made to control the oil temperature other than to ensure that it was constant during each run.

Before performing the nonsynchronous perturbation runs, data from a startup was obtained in order to study the whirl threshold and whip transitions. The results of that startup are shown in a full spectrum cascade plot (Figure 2). The rotor speeds that were selected for the nonsynchronous perturbation experiments are shown in red. These were 1000 rpm, 1450 rpm, and 1900 rpm in the stable region, 2275 rpm in the stable region at the edge of fluid-induced instability, 2525 rpm in whirl, and 5000 rpm in whip.

The nonsynchronous perturbations were performed using the following procedure. After checking the journal centering in the bearing, the rotor was set to operate at the desired speed (for example, 1000 rpm). For the stable runs, the perturbator motor was ramped slowly from 250 cpm to 2500 cpm. Vibration data was obtained from a pair of XY eddy current transducers located in the fluid bearing shell. These signals were sent to an ADRE® for Windows (Automated Diagnostics for Rotating Equipment) System and were filtered to the perturbation frequency.

For the whirl and whip cases, the perturbation frequency was set by hand at 50 cpm intervals. The signal from the vertical bearing transducer was filtered using a special high gain, narrow bandpass filter with a long time constant (typically 100 s or 300 s). This special filter was necessary to extract the relatively small perturbation signal from the large whirl or whip vibration signal. For these special cases, to allow the filter to settle, the time between data points ranged from 10 minutes to as long as 30 minutes.

The filtered amplitude and phase data from the 1000 rpm run is shown in Figure 3. Note that the force was located at the vertical transducer (0°) when the Keyphasor event occurred. Note also that the low speed response phase leads the force at low speeds. This is typical behavior for a rotor system with high Quadrature Stiffness undergoing nonsynchronous perturbation.

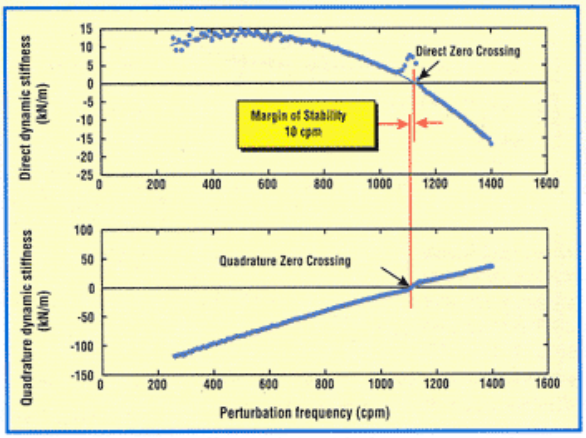

Figure 7. Dynamic Stiffness plots with the rotor operating at 2275 rpm, slightly below the Threshold of Stability. The Margin of Stability has decreased to 10 cpm.

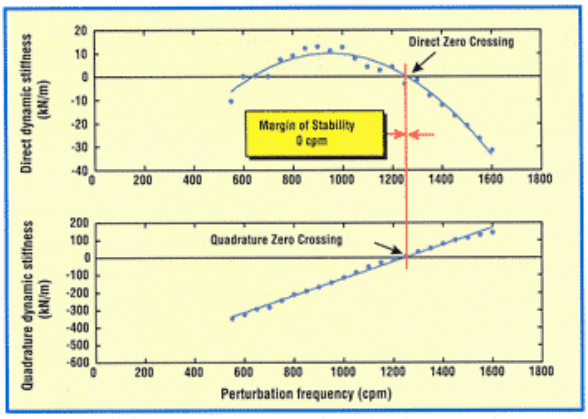

Figure 8. Dynamic Stiffness plots with the rotor operating in oil whirl at 2525 rpm. Rotor dynamic eccentricity ratio is 0.75. The Direct and Quadrature Dynamic Stiffnesses both cross zero at the same frequency, which is the whirl frequency of 1220 cpm. The Margin of Stability is zero.

The Dynamic Stiffness was calculated for each speed in each run using the following basic relationship:

$$\vec{K}_{DS} = \frac{\vec{F}}{\vec{R}} \qquad (3)$$

where $\vec{F}$ is the force, and $\vec{R}$ is the filtered rotor response. This is just a different form of Equation (2). The Dynamic Stiffness was then separated into Direct and Quadrature parts (mathematically called Real and Imaginary, although there is nothing "imaginary" about the Quadrature Stiffness!). The experimental Direct Dynamic Stiffness data was then fit to a parabolic curve,

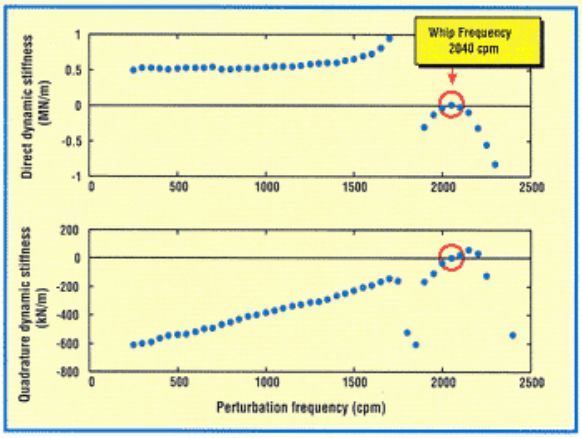

Figure 9. Dynamic Stiffness plots with the rotor operating in oil whip at 5000 rpm. Rotor dynamic eccentricity ratio is 0.85. No curve fits were performed. At the whip frequency of 2040 cpm, the measured Direct and Quadrature Dynamic Stiffnesses are both zero. These points are circled in red.

and the Quadrature Dynamic Stiffness was fit to a straight line. The Dynamic Stiffness data was then plotted together with the curve fits. These plots are shown in Figures 4 through 8.

Discussion of results

The first thing to notice is the behavior of the rotor system when operating in the stable region. Figures 4, 5, 6, and 7 show the Dynamic Stiffness plots for the nonsynchronous runs conducted while the rotor was running at 1000 rpm, 1450 rpm, 1900 rpm, and 2275 rpm, respectively. Note that, in Figure 4, the Direct Dynamic Stiffness (the top graph) crosses the axis (the zero crossing) at approximately 840 cpm, while the Quadrature Dynamic Stiffness (the lower graph) crosses zero at approximately 480 cpm. The frequency separation between these two zero crossings represents the *Margin of Stability*, which is approximately 360 cpm for this case. Remember that fluid-induced instability will occur when both the Direct and the Quadrature Dynamic Stiffnesses are zero *at the same frequency*. A non-zero Margin of Stability indicates that the machine is not subject to fluid-induced instability at that operating speed.

Figure 5 shows that, with the rotor running at 1450 rpm, the Margin of Stability has decreased to 230 cpm. Figure 6 shows that, at 1900 rpm, the Margin of Stability has been reduced to 80 cpm. These plots clearly show that, as the rotor speed begins to approach the Threshold of Stability, the Margin of Stability decreases. Figures 4, 5, and 6 clearly show the Direct and Quadrature zero crossings moving closer together.

Figure 7 shows the Dynamic Stiffness of the rotor system when it is operating at 2275 rpm, very close to the onset of fluid-induced instability. The Margin of Stability is only 10 cpm at this speed. However, the rotor is stable, and the non-zero Margin of Stability reflects this fact.

The onset of fluid-induced instability (oil whirl) occurred at a speed only slightly above 2275 rpm. The rotor speed was increased to 2525 rpm, which was well into the whirl region. Measurements of the whirl orbit at this speed showed the dynamic eccentricity ratio to be 0.75. In other words, the orbit diameter was 75% of the available bearing clearance. Figure 8 shows the Dynamic Stiffness of the rotor system while it was operating in oil whirl at 2525 rpm. During this run, the oil film in the bearing was observed to be intact; that is, the journal and bearing were fully lubricated at all times.

Note that the Direct and Quadrature zero crossings for the whirl case occur at the *same frequency*, and the Margin of Stability is zero. The frequency at which the two curve fits have their zero crossing is approximately 1250 cpm. Given the noise in the data, this is in very good agreement with the measured oil whirl frequency of 1220 cpm. The rotor is whirling at its natural frequency.

As the rotor speed was increased to 5000 rpm, the subsynchronous whip frequency became nearly constant with rotor speed. This can be seen in the full spectrum cascade plot (Figure 2). At 5000 rpm, the oil film in the bearing was observed to be mostly intact, with only a few small circumferential streaks. These streaks indicated that a small amount of air was being pulled into the bearing. At this speed, the measured dynamic eccentricity ratio of the whip orbit was 0.85. The higher oil temperature of 44° C (111° F) in whip, compared to 27° C (81° F) in whirl, indicates that the oil film was being sheared much more strongly in whip.

Data collection from nonsynchronous perturbation in whip was not obtained as easily as the previous run in whirl. There was considerably more difficulty in extracting steady, filtered, perturbation response data. This was primarily due to the fact that the very high bearing stiffness at this high, dynamic eccentricity ratio (0.85) resulted in a very small rotor response to the perturbation force. In addition, it appears that the basic rotor behavior may have changed, showing evidence of another mode. Figure 9 shows the measured Dynamic Stiffness of the rotor system in whip. The rotor system behavior no longer fits the simple rotor system model that was used before, so it is not possible to fit a meaningful curve to the data. However, in spite of that, it can be seen that the two data points at the whip frequency of 2040 cpm (circled in red) show that the Direct and Quadrature Stiffnesses are both zero *at the whip frequency.*

What do these results mean? First, in both whirl and whip, it is clear from the data that the rotor system is

operating with a Margin of Stability of zero *at the Threshold of Stability.* This is demonstrated by the fact that both the Direct and Quadrature Dynamic Stiffnesses are zero at the whirl or whip frequency.

This can also be illustrated by a Root Locus plot [3]. Figure 10 shows a Root Locus plot of the rotor system under test. The operating points on the plot were obtained by first obtaining rotor parameters from the Dynamic Stiffness curve fits and applying them to a rotor model that included the Fluid Inertia Effect [4]. For the whip data, the Root Locus point could not be determined from a model, so it was plotted based on observed behavior. The Root Locus plot displays the experimental rotor system natural frequency on the vertical axis versus a growth or decay factor on the horizontal axis. The entire right half-plane represents an operating region where rotor system is forbidden, that is, rotor vibration, once it started, would increase in amplitude forever. For normal, stable operation, the rotor system must operate in the left half-plane.

In Figure 10, note that the operating points for stable operation are in the left half-plane. The operating points for whirl and whip are located *on the vertical axis*, and the natural frequency of the rotor system *is the same as the whirl and whip frequency*. Thus, in whirl and whip the rotor system is at the Threshold of Stability and it is precessing *at the rotor system natural frequency*.

Summary

These experiments have demonstrated that the Margin of Stability steadily decreases as the rotor speed approaches the Threshold of Stability. As the rotor enters unstable operation, it starts whirling or whipping at its natural frequency. In both whirl and whip, the Dynamic Stiffness zero crossings occur at the frequency of the whirl or whip.

We can conclude that a rotor system operating in a fluid instability will have zero Direct and zero Quadrature Dynamic Stiffness at the frequency of the instability.

References

1. Bently, D. E., "Fluid Circumferential Average Velocity Ratio a Key Factor in Rotor/Bearing/Seal Models," Orbit, Bently Nevada Corporation, v. 8, No. 1, February 1987.
2. Bently, D. E., Muszynska, A., "Perturbation Study of a Rotor/Bearing System: Identification of the Oil Whirl and Oil Whip Resonances," Tenth ASME Design Engineering Division Conference on Mechanical Vibration and Noise, Paper 85-DET-142, Cincinnati, Ohio, September 1985.
3. Bently, D. E., Hatch, C. T., "Root Locus and the Analysis of Rotor Stability Problems," Orbit, Bently Nevada Corporation, v. 14, No. 4, December 1993.
4. Muszynska, A., and Bently, D. E., "Frequency-Swept Rotating Input Perturbation Techniques and Identification of the Fluid Force Models in Rotor/Bearing/Seal Systems and Fluid Handling Machines," Journal of Sound and Vibration, v. 143, No. 1, 1990, pp. 103-124.

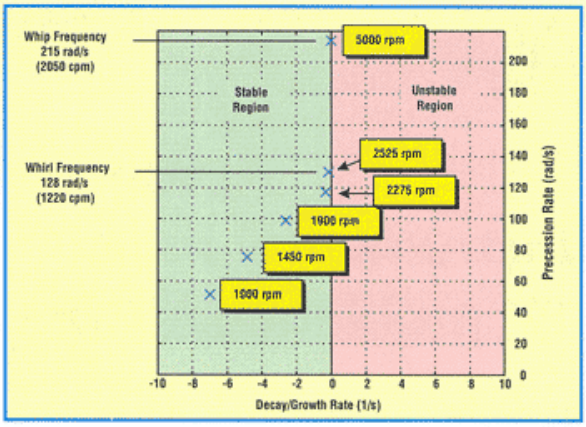

Figure 10. Root Locus plot of the operating points in the experiments. This graph plots Decay/Growth rate on the horizontal axis versus rotor system natural frequency on the vertical axis. Stable rotor operation plots in the left half-plane. Rotor operation in the right half-plane is forbidden, since it would imply unlimited rotor vibration amplitude. The rotor operation, stable at speeds of 1900 rpm and below, plots very close to the vertical axis at 2275 rpm. The rotor in whirl at 2525 rpm is precessing at the Low Eccentricity Natural Frequency, while in whip at 5000 rpm it is precessing at the High Eccentricity Natural Frequency.

The difference between whirl and whip

Obviously, there is a difference between the behavior of the rotor system in whirl versus its behavior in whip. To understand why this is so, it is first necessary to realize that the rotor system direct stiffness K, actually consists of a combination of the shaft spring and the bearing spring. (There can be additional stiffness contributions from other sources, but for the purposes of this article we can neglect them.) The shaft spring stiffness is effectively in series with the bearing spring. When two springs are in series, then the weakest spring controls the overall stiffness of the combination.

At the onset of whirl, the rotor was operating in the center of the bearing where the bearing spring stiffness (which increases strongly near the bearing wall) was minimum. The rotor system stiffness was controlled by the weaker bearing stiffness. Thus, the natural frequency of the rotor system was at a minimum, which is called the *Low Eccentricity Natural Frequency* (Figure 2). As the rotor starts into whirl, the diameter of the orbit and the bearing stiffness increased. This stiffness increase changed the zero point of the Direct Dynamic Stiffness slightly. Thus, the stiffness increase keeps the rotor system on the edge of the stability threshold and prevents the orbit diameter from increasing. The natural frequency of the rotor also increases slightly. This holds true as long as the rotor speed remains the same. If, however, the rotor speed increases, the rotor exceeds the new Threshold of Stability, the orbit diameter increases, and the cycle repeats. Thus, in whirl, it is the changing bearing spring stiffness that keeps increasing the natural frequency of the rotor system, and the whirl frequency tracks along an order line on the spectrum cascade plot as rotor speed increases. This order line is approximately λX.

However, at some point, the bearing spring stiffness becomes so high that it is no longer the weakest spring in the rotor system. The shaft spring is now the weakest spring, and the shaft spring cannot be modified. Thus, the rotor system asymptotically approaches what we call the *High Eccentricity Natural Frequency* (Figure 2). In this region, the subsynchronous frequency of precession of the rotor system remains constant, and we define this instability region as whip. It is this frequency that often correlates with the "nameplate critical" in rotating machinery.